ChemComm

Accepted Manuscript

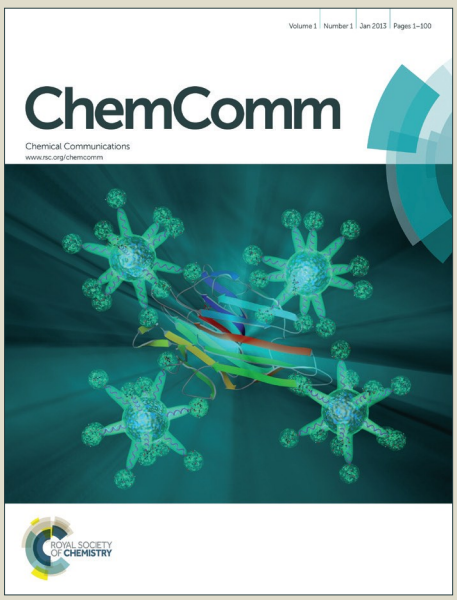

ROYAL SOCIETY OF CHEMISTRY

www.rsc.org/chemcomm

Dynamic Response of a Flexible Indium Based Metal-Organic Framework to Gas Sorption†

Xingjun Li, Xueyuan Chen, Feilong Jiang, Lian Chen, Shan Lu, Qihui Chen, Mingyan Wu, Daqiang Yuan and Maochun Hong*

Received (in XXX, XXX) Xth XXXXXXXXX 201X, Accepted Xth XXXXXXXXX 201X
First published on the web Xth XXXXXXXXX 201X
DOI: 10.1039/b000000x

A doubly interpenetrated microporous indium based metal-organic framework was solvothermally synthesized, in which cage-like pores and one-dimensional channels coexist. Due to its flexible nature, the complex exhibits a novel dynamic response to N_2, Ar and CO_2 sorption. Furthermore, the material shows a high H_2 uptake capacity.

During the past few decades, porous metal-organic frameworks (MOFs) have attracted great attention not only because of their fascinating architectures[1] but also due to their exploitable properties for potential applications in gas storage and separation,[2] ion exchange,[3] chemical sensor,[4] drug delivery,[5] proton conduction,[6] catalysis,[7] *etc*. Compared with other solid physisorbents, such as porous zeolites and carbon materials, these metal-organic hybrid materials generally incorporate both metal centers and polyfunctional organic ligands, with large pore volume for gas storage. The porous MOFs were classified into three categories according to different structural responses of the host frameworks to gas storage: (i) the first-category materials are comparably labile and collapse irreversibly after the removal of the gas molecules; (ii) the second-category compounds have stable and robust frameworks, which maintain the original porous structures before and after guest sorption; (iii) the third-category compounds have flexible porous frameworks, which exhibit dynamic response to gas sorption.[8] Whereas recent developments on self-assembly of coordination complexes have provided many rigid porous MOFs with excellent gas sorption properties, flexible or dynamic MOFs are still under development and they are attracting more and more attention for their special applications, such as selective separation, chemical sensing, controlled drug storage and delivery, and even hazardous waste adsorption.[9]

One of fascinating properties for flexible MOFs is so-called breathing effect which can be triggered by different external stimulus, including gas sorption, temperature, pressure, *etc*.[10] It is well-known that the most studied breathing MOFs are MIL-53 and its analogues, which show reversible breathing behaviour upon the CO_2 sorption.[11] Due to their numerous potential applications, breathing MOF arouse more and more research interest and a number o methodologies have been developed for the synthesis of th materials. A large number of breathing MOFs come from pillared layer coordination polymers, which commo compose of a rigid layer as the solid roof and flexible ligands as expandable pillars or swiveling linkers. Another source of breathing MOFs can arise from interpenetrated MOFs, i which weak interactions such as hydrogen bonds and π-π interactions play an important role in the dynamic behaviou of the framework.[12]

In this work, we present a new three-dimensional flexi indium based MOF $In(TCPBDA)(MeNH_3)\cdot 6H_2O$ (denoted a complex **1**). Complex **1** exhibits a doubly interpenetrate microporous framework with one-dimensional rhombic channels. It is interested that the material demonstrates a nove dynamic sorption behaviour upon N_2, Ar and CO_2 uptakes. As far as we are aware, complex **1** represents the firs example of indium based MOFs with an irreversible dynamic response to gas sorption.

Colorless block crystals of complex **1** were obtained by a solvothermal reaction between $H_4TCPBDA$ and $InCl_3\cdot 4H_2O$ in *N,N'*-dimethylformamide (DMF) with an additional HCl a

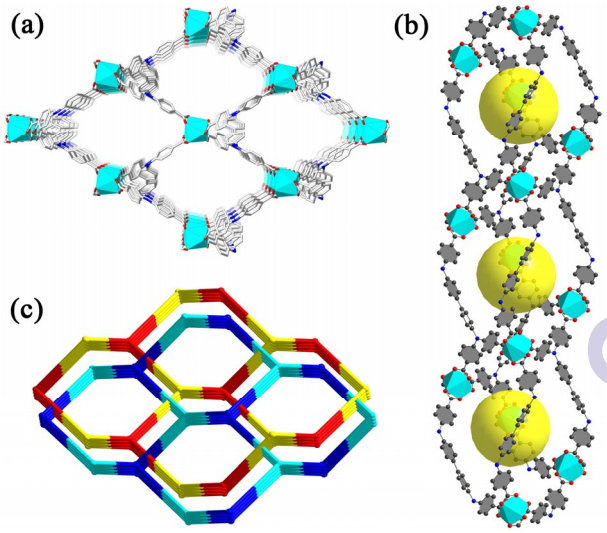

Fig. 1 Three-dimensional open framework along the *b*-axis (a), cage-like pores (b) and the two-fold interpenetrating neb topology (c) of complex **1**.

Key Laboratory of Optoelectronic Materials Chemistry and Physics, and Key Laboratory of design and assembly of functional nano-structures, Fujian Institute of Research on the Structure of Matter, Chinese Academy of Sciences, Fuzhou, 350002, China.
E-mail: *hmc@fjirsm.ac.cn*.
Tel: +86-591-63173966; Fax: +86-591-63173068.
†Electronic supplementary information (ESI) available: Synthesis, crystallographic information, supplementary figures, IR, PXRD, TGA and sorption results of complexes **1** and **1a**. For ESI and crystallographic data in CIF or other electronic format see DOI: 10.1039/b000000x.

120 °C for three days (see ESI† for details) (H_4TCPBDA = *N,N,N',N'*-tetrakis(4-carboxyphenyl)-biphenyl-4,4'-diamine). The phase purity of above block product has been confirmed by powder X-ray diffraction (PXRD) (Fig. S5, ESI†). X-Ray crystallography reveals that complex **1** crystallizes in the monoclinic system with space group *C2/c*. The asymmetrical unit of complex **1** contains one independent In(III) ion and one fully deprotonated TCPBDA^{4-} ligand. In this structure, we assume that the distorted $MeNH_3^+$ cations, which are the byproduct of *in situ* decomposition of the DMF solvent, lie inside the accessible void, thus leading to the charge equilibrium.[13] Every In(III) atom is typically eight-coordinated by eight carboxylate oxygen atoms from four TCPBDA^{4-} ligands giving a tetrahedral four-connected node (Fig. S2, ESI†). Each TCPBDA^{4-} ligand connects to four In(III) ions using its four carboxylate groups, with the observed In-O bond lengths in the range of 2.182(3)-2.468(4) Å (Table S2, ESI†). The phenyl rings around the nitrogen atoms in TCPBDA^{4-} are tilted towards each other, with the dihedral angles of 59.37° and 63.04°, respectively. Moreover, the two central phenyl rings in each ligand are not coplanar with a dihedral angle of 38.81°. Structurally speaking, complex **1** presents a three-dimensional network constructed from the [In(O_2CR)$_4$] units and the tetracarboxylate ligands with one-dimensional rhombic channels along the *b*-axis. It is noteworthy that there are cage-like pores in the structure of complex **1** along the *a*-axis (Fig. 1b). From the viewpoint of topology, we can simplify both the [In(O_2CR)$_4$] units and the TCPBDA^{4-} ligands as four-connected nodes. As a result, complex **1** adopts a diamond-like four-connected uninodal net with a topological point symbol of {6^6} (Fig. 1c).

The free volume of complex **1** with removal of gust solvent molecules is 62.5% calculated by PLATON (1.8 Å probe radius). To study the porosity of complex **1**, the N_2 physisorption measurement was performed at 77 K. For this purpose the synthesized material was washed with DMF, followed by an exchange of the guest solvent with absolute acetone for one week. Interestingly, we discovered an unusual sorption behaviour for complex **1**. The N_2 physisorption measurement reveals two steps in the adsorption branch of the isotherm (Fig. 2a). The adsorption branch of the isotherm begins at relatively low uptake. Up to a relative pressure of 0.57 the observed isotherm corresponds to a classical type-I isotherm reaching the plateau at about 27.49 cm^3g^{-1}. To our surprise, the relative pressure declines rapidly to 0.41 in the isotherm, meanwhile, the amount of N_2 adsorption suddenly rises to 256.78 cm^3g^{-1}. This interesting adsorption behaviour reveals that a gate-opening effect occurs in the framework at a relative pressure of 0.57, giving rise to a significant volume increase. The isotherm reaches saturation at 391.63 cm^3g^{-1}. It should be noted that the desorption trace of the isotherm does not follow the adsorption branch, especially in the low pressure region, giving a large hysteresis loop to the isotherm. We propose that the material undergoes a structural transition from the narrow pore (**np**) form to the large pore (**lp**) form induced by the N_2 adsorption. The host-guest interactions give rise to large pressure on the pore walls, resulting in the expanded pores. In following sorption experiment, we try to verify the cyclability of the desolvated material. We record the second cycle of N_2 sorption at 77 K without the reactivation process after the first cycle. Upon the second cycle, the material exhibits a reversible type-I isotherm, a characteristic of microporous materials, with saturated N_2 uptake of 380.98 cm^3g^{-1} at 77 K, corresponding to BET and Langmuir surface area of 1468.37 m^2g^{-1} and 1647.51 m^2g^{-1}, respectively. Furthermore, a second cycle N_2 sorption with the reactivated sample displays a similar type-I isotherm with a N_2 uptake of 391.77 cm^3g^{-1} (Fig. S9, ESI†). Hence, the second cycle N_2 sorption measurement shows that complex **1** clearly remains in the **lp** form and displays a type-I sorption isotherm. In contrast to the materials with breathing effect, *e.g.* MIL-53, complex **1** presents an irreversible dynamic response to N_2 sorption.

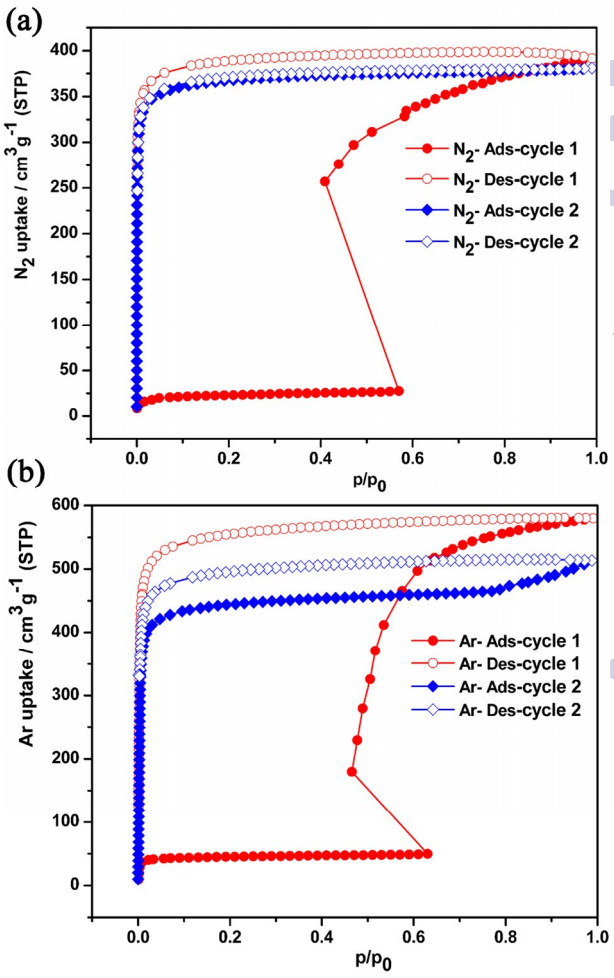

Fig. 2 Experimental N_2 (a) and Ar (b) sorption isotherm at 77 K and 87 K for complex **1**.

To confirm the dynamic sorption behaviour of complex **1**, the Ar sorption measurement is performed at 87 K. As shown in Fig. 2b, Ar sorption for complex **1** exhibits a similar isotherm with that of N_2 sorption. A classical type-I isotherm has been observed at the first step until the relative pressure reaches 0.63 with an Ar adsorption of 49.71 cm^3g^{-1}. Then the relative pressure rapidly declines to 0.46. Meanwhile, the

amount of Ar adsortion increases to 179.75 cm^3g^{-1}. Finally, the Ar uptake rises to 579.76 cm^3g^{-1} at 0.99 bar. Likewise, the desorption trace of the isotherm does not follow the adsorption branch, giving a large hysteresis loop. The second cycle of Ar sorption displays a type-I sorption isotherm with a Ar uptake of 513.37 cm^3g^{-1} at 0.99 bar. The above results show that complex **1** exhibits a dynamic response to Ar sorption as well. In addition, we also investigate CO_2 and CH_4 sorptions for complex **1** at 273 and 295 K. The sorption isotherms show a CO_2 uptake of 78.98 cm^3g^{-1} and a CH_4 uptake of 17.43 cm^3g^{-1} (Fig. S10, ESI†). It is noteworthy that the dynamic sorption behaviour could not be observed for CO_2 and CH_4 uptakes at 273 and 295 K. The different gas sorption behaviours for CO_2 and CH_4 can be possibly attributed to the higher experimental temperature than that of N_2 and Ar or different affinities between these gas molecules and the host framework.[8,14] To confirm the influence of the experimental temperature, the CO_2 and CH_4 isotherms are measured at a lower temperature of 195 K (isopropanol/dry ice bath). As expected, a hysteresis loop can be observed in the CO_2 isotherm, showing a dynamic response to CO_2 sorption for complex **1** (Fig. 3). The saturated CO_2 adsorption is up to 181.42 cm^3g^{-1}. The second cycle of CO_2 sorption at 195 K exhibits a type-I sorption isotherm without any hysteresis, suggesting an irreversible dynamic response for the complex (Fig. S11, ESI†). In contrast, the CH_4 sorption at 195 K displays a similar isotherm with that measured at 273 K (Fig. S12, ESI†).

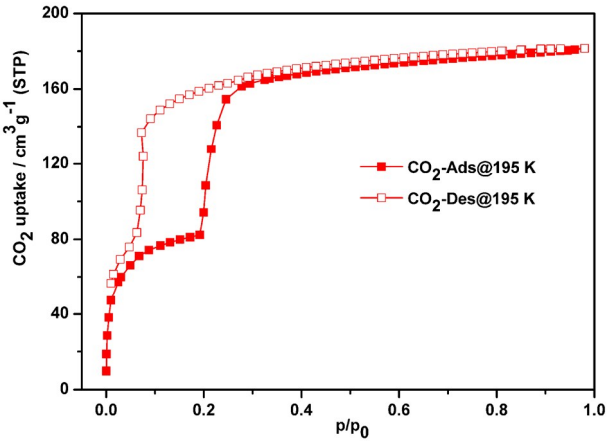

Fig. 3 Experimental CO_2 sorption isotherm at 195 K for complex **1**.

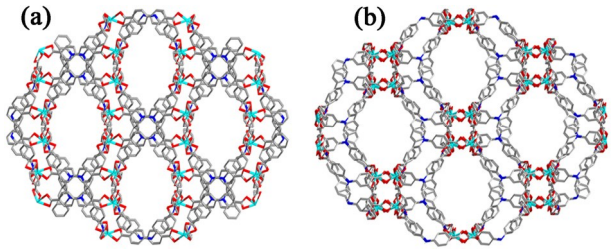

Fig. 4 Views of porous framework structures for complexes **1** (a) and **1a** (b) along the *c*-axis, showing a pore expansion upon N_2 sorption.

Although single crystals of complex **1** tend to crack during gas sorption process, we were successful in obtaining the single-crystal structure of complex **1** after N_2 sorption (denoted as complex **1a**). To reveal more details for the dynamic behaviour upon gas sorption, the structures of complexes **1** and **1a** were carefully compared. The bond lengths and angles of the $[In(O_2CR)_4]$ units and the surrounding carboxylate donors are almost unchanged (Table S2 and Table S3, ESI†). The changes occurred in the $TCPBDA^{4-}$ ligand consisting of many freely rotated C-C and C-N single bonds. The aromatic rings significantly rotated around the ligand scaffold, which can be judged by the largely varied dihedral angles between the central phenyl rings (38.81° in complex **1** and 22.69° in complex **1a**) and the ones surrounding the carboxylate donors (59.37° and 63.04° in complex **1** and 62.45° and 72.26° in complex **1a**). Moreover, the C-N-C angles of the ligand reduced from 122.88° and 124.06° in complex **1** to 119.90° and 120.82° in complex **1a**, respectively, suggesting a swing occurred for the four terminal arms of the ligand. The above conformational changes of the organic ligand result in a shape diversion to the independent network for the compl... It is noteworthy that a significant shifting transition occurred for the adjacent networks in complex **1** upon gas sorption (Fig. S3, ESI†). A pore expansion was finally achieved for the complex upon gas sorption (Fig. 4). The structural transform can be further confirmed by the changes between the powder X-ray diffraction (PXRD) patterns of complexes **1** and **1a** (Fig. S5, ESI†). We propose that the steric constraints and molecular interactions between the adjacent networks endow complex **1a** with a stable structure. Thus the doubly interpenetrated structure may be the main reason for the irreversible sorption behaviour for complex **1** which is different from MIL-53 possessing an uninterpenetrated framework.[11]

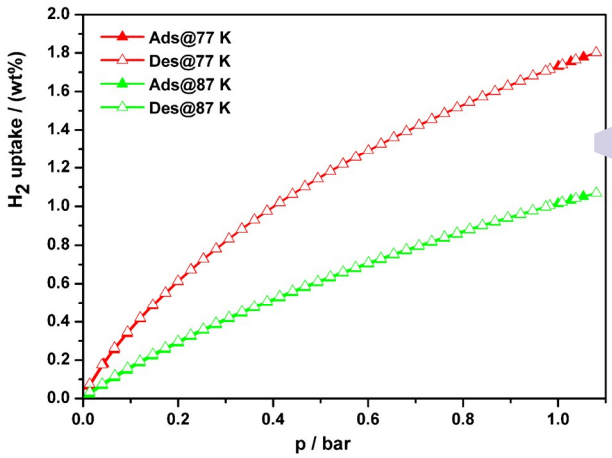

Fig. 5 H_2 uptake for complex **1** measured at 77 K and 87 K.

Meanwhile, we investigate the volumetric hydrogen sorption capacity of complex **1** at 77 and 87 K (Fig. 5). All the H_2 isotherms show rapid kinetics and good reversibility without any hysteresis. The H_2 uptake capacity is up to 201.9 cm^3g^{-1}(1.80 wt%) at 77 K and 1.08 bar, and 120 cm^3g^{-1}(1.0... wt%) at 87 K and 1.08 bar. These experimentally obtained values in hydrogen capacity are comparable to those well known microporous MOF materials under the same

measurement conditions. Moreover, the adsorption heat of hydrogen (Q_{st}) is simulated by the Clausius-Clapeyron equation and its value at zero coverage for complex **1** is calculated to be 5.72 kJ mol^{-1}, and drops gradually with the incremental H_2 loading (Fig. S15, ESI†). In this case, we attribute most of the H_2 loading capacity to the intrinsically large guest-accessible volume, especially the large cage-like pores and opening channels.

In conclusion, a doubly interpenetrated microporous indium based metal-organic framework has been synthesized and structurally characterized. In the presented structure, the $[In(O_2CR)_4]$ subunits are linked by the tetracarboxylate ligands to form a highly porous framework with the coexistence of microporous cages and one-dimensional channels. Due to its flexible nature, complex **1** displays an irreversible dynamic response to N_2, Ar and CO_2 sorption. The structure of complex **1a** reveals that conformational changes of the ligand and significant shifting transitions of the adjacent networks occurred for complex **1**, resulting in a pore expansion upon gas sorption. The doubly interpenetrated structure of complex **1** plays an important role for the irreversible gas sorpton behaviour. It is expected that this work might motivate more extensive research on the responsive properties of flexible frameworks.

We are grateful for financial support from the 973 Program (2013CB933200), the National Natural Foundation of China (21131006, 21401196, 21201163) and the Natural Science Foundation of Fujian Province.

Notes and references

Crystal data for complex **1** (CCDC 982263): $C_{40}H_{24}N_2O_8In$, M = 775.43, monoclinic, space group $C2/c$, a = 28.286(4), b = 20.942(3), c = 27.586(1) Å, β = 120.80°, V = 14037(2) Å^3, Z = 8, D_c = 0.734 g/cm^3, F_{000} = 3128, CuKα radiation, λ = 1.54184 Å, T = 100(2) K, $2\theta_{max}$ = 73.5°, 42886 reflections collected, 13842 unique (R_{int} = 0.040). Final *GooF* = 1.009, R_1 = 0.0597, wR_2 = 0.1928, R indices based on 9682 reflections with I >2sigma(I) (refinement on F^2). Crystal data for complex **1a** (CCDC 1435243): $C_{40}H_{24}N_2O_8In$, M = 775.43, monoclinic, space group $I2/c$, a = 26.9793(6), b = 21.3292(4), c = 26.4721(5) Å, β = 97.00°, V = 15119(5) Å^3, Z = 8, D_c = 0.681 g/cm^3, F_{000} = 4496, CuKα radiation, λ = 1.54184 Å, T = 100(2) K, $2\theta_{max}$ = 73.5°, 14694 reflections collected, 11291 unique (R_{int} = 0.039). Final *GooF* = 1.071, R_1 = 0.0587, wR_2 = 0.1792, R indices based on 11291 reflections with I >2sigma(I) (refinement on F^2). The diffraction data for complexes **1** and **1a** were treated by the ''*SQUEEZE*'' method as implemented in PLATON[15] to remove diffuse electron density associated with the badly disordered solvent molecules. The final formula of complex **1** was determined by combining with thermogravimetric analysis (TGA) and elemental analyses.

1. (a) M. Eddaoudi, D. F. Sava, J. F. Eubank, K. Adil and V. Guillerm, *Chem. Soc. Rev.*, 2015, **44**, 228; (b) Y. B. Zhang, H. Furukawa, N. Ko, W. Nie, H. J. Park, S. Okajima, K. E. Cordova, H. Deng, J. Kim and O. M. Yaghi, *J. Am. Chem. Soc.*, 2015, **137**, 2641; (c) J. R. Li, J. Sculley and H. C. Zhou, *Chem. Rev.*, 2012, **112**, 869; (d) J. P. Zhang, Y. Y. Lin, X. C. Huang and X. M. Chen, *J. Am. Chem. Soc.*, 2005, **127**, 5495.
2. (a) S. H. Yang, J. L. Sun, A. J. Ramirez-Cuesta, S. K. Callear, W. I. F. David, D. P. Anderson, R. Newby, A. J. Blake, J. E. Parker, C. C. Tang and M. Schroder, *Nat. Chem.*, 2012, **4**, 887; (b) W. G. Lu, D. Q. Yuan, T. A. Makal, J. R. Li and H. C. Zhou, *Angew. Chem, Int. Ed.*, 2012, **51**, 1580; (c) D. Banerjee, A. J. Cairns, J. Liu, R. K. Motkuri, S. K. Nune, C. A. Fernandez, R. Krishna, D. M. Strachan and P. K. Thallapally, *Acc. Chem. Res.*, 2015, **48**, 211; (d) B. Liu, M. Tu and R A. Fischer, *Angew. Chem, Int. Ed.*, 2013, **52**, 3402.
3. (a) L. Gao, C. V. Li, K. Y. Chan and Z. N. Chen, *J. Am. Chem. Soc.*, 2014, **136**, 7209; (b) B. Q. Song, X. L. Wang, Y. T. Zhang, X. S. Wu, H. S. Liu, K. Z. Shao and Z. M. Su, *Chem. Commun.*, 2015, **51**, 9515; (c) J. S. Qin, S. R. Zhang, D. Y. Du, P. Shen, S. J. Bao, Y. Q. Lan and Z. M. Su, *Chem. Eur. J.*, 2015, **20**, 5625; (d) Z. J. Zhang, W. Shi, Z. Niu, H. H. Li, B. Zhao, P. Cheng, D. Z. Liao and S. P. Yan, *Chem. Commun.*, 2011, **47**, 6425.
4. (a) Z. Hu, B. J. Deibert and J. Li, *Chem. Soc. Rev.*, 2014, **43**, 5815; (b) Z. Q. Shi, Z. J. Guo and H. G. Zheng, *Chem. Commun.*, 2015, **51**, 8300; (c) Y. Yang, F. Jiang, L. Chen, J. Pang, M. Wu, X. Wan, J. Pan, J. Qian and M. Hong, *J. Mater. Chem. A,* 2015, **3**, 13526; (d) M. Zhang, G. Feng, Z. Song, Y.-P. Zhou, H.-Y. Chao, D. Yuan, T. T. Y. Tan, Z. Guo, Z. Hu, B. Z. Tang, B. Liu and D. Zhao, *J. Am. Chem. Soc.*, 2014, **136**, 7241.
5. (a) J. D. Rocca, D. Liu and W. Lin, *Acc. Chem. Res.,* 2011, **44**, 957; (b) J. Zhuang, C.-H Kuo, L.-Y. Chou, D.-Y. Liu, E. Weerapana and C.-K. Tsung, *ACS Nano*, 2014, **8**, 2812; (c) C. He, K. Lu, D. Liu and W. Lin, *J. Am. Chem. Soc.*, 2014, **136**, 5181.
6. (a) M. Sadakiyo, T. Yamada and K. Kitagawa, *J. Am. Chem. Soc.*, 2014, **136**, 13166; (b) Y. Ye, L. Zhang, Q. Peng, G.-E. Wang, Y Shen, Z. Li, L. Wang, X. Ma, Q.-H. Chen, Z. Zhang and S. Xiang, *J. Am. Chem. Soc.*, 2015, **137**, 913; (c) T. Yamada, K. Otsubo, F Makiura and H. Kitagawa, *Chem. Soc. Rev.*, 2013, **42**, 6655.
7. (a) M. Yoon, R. Srirambalaji and K. Kim, *Chem. Rev.*, 2012, **112**, 1196; (b) K. Manna, T. Zhang, F. X. Greene and W. Lin, *J. Am Chem. Soc.*, 2015, **137**, 2665; (c) J. Zheng, M. Wu, F. Jiang, W. Su and M. Hong, *Chem. Sci.,* 2015, **6**, 3466; (d) C. M. McGuirk, M. J. Katz, C. L. Stern, A. A. Sarjeant, J. T. Hupp, O. K. Farha and C. A. Mirkin, *J. Am. Chem. Soc.*, 2015, **137**, 919; (e) Q.-L. Zhu, J. Li and Q. Xu, *J. Am. Chem. Soc.*, 2013, **135**, 10210.
8. S. Horike, S. Shimomura and S. Kitagawa, *Nat. Chem.*, 2009, **1**, 695.
9. (a) Z. Wang and S. M. Cohen, *J. Am. Chem. Soc.*, 2009, **131**, 16675; (b) C. R. Murdock, N. W. McNutt, D. J. Keffer and D. M. Jenkins, *J. Am. Chem. Soc.*, 2014, **136**, 671.
10. G. Férey and C. Serre, *Chem. Soc. Rev.*, 2009, **38**, 1380.
11. (a) C. Serre, F. Millange, C. Thouvenot, M. Noguès, G. Marsolier, D. Louër and G. Férey, *J. Am. Chem. Soc.*,2002, **124**, 13519; (b) C. Serre, S. Bourrelly, A. Vimont, N. A. Ramsahye, G. Maurin, P. L. Llewellyn, M. Daturi, Y. Filinchuk, O. Leynaud, P. Barnes and G. Férey, *Adv. Mater.*, 2007, **19**, 2246; (c) P. L. Llewellyn, G. Maurin, T. Devic, S. Loera-Serna, N. Rosenbach, C. Serre, S. Bourrelly, P. Horcajada, Y. Filinchuk and G. Férey, *J. Am. Chem. Soc.*,2008, **130**, 12808; (d) N. A. Ramsahye, G. Maurin, S. Bourrelly, P. L. Llewellyn T. Loiseau, C. Serre and G. Férey, *Chem. Commun.*, 2007, 3261.
12. (a) S. Yang, X. Lin, W. Lewis, M. Suyetin, E. Bichoutskaia, J. E. Parker, C. C.Tang, D. R. Allan, P. J. Rizkallah, P. Hubberstey, N. R. Champness, K. M. Thomas, A. J. Blake and M. Schröder, *Nat. Mater.*, 2012, **11**, 710; (b) C. R. Murdock, N. W. McNutt, D. J. Keffer and D. M. Jenkins, *J. Am. Chem. Soc.*,2014, **136**, 671; (c) A. Schneemann, S. Henke, I. Schwedler and R. A. Fischer, *ChemPhysChem*, 2014, **15**, 823; (d) Y.-S. Wei, K.-J. Chen, P.-Q. Liao, B.-Y. Zhu, R.-B. Lin, H.-L. Zhou, B.-Y. Wang, W. Xue, J.-P. Zhang and X.-M. Chen, *Chem. Sci.*, 2013, **4**, 1539; (e) S. Henke, A. Schneemann, A. Wütscher and R. A. Fischer, *J. Am. Chem. Soc.*, 2012, **134**, 9464.
13. S.-T. Zheng, J. J. Bu, T. Wu, C. Chou, P. Feng and X. Bu, *Angew. Chem, Int. Ed.*, 2011, **50**, 8858.
14. K. L. Gurunatha and T. K. Maji, *Inorg. Chem.*, 2009, **48**, 10886.
15. (a) A. L. Spek, *J. Appl. Crystallogr.*, 2003, **36**, 7; (b) P. V. D. Sluis and A. L. Spek, *Acta Crystallogr., Sect. A*, 1990, **46**, 194.